Hindawi
Advances in Condensed Matter Physics
Volume 2022, Article ID 7740210, 9 pages
https://doi.org/10.1155/2022/7740210

Research Article

Study on the Adsorption Characteristics of Mo-Doped Graphene on the Decomposition Products of SF_6 Substitute Gas Based on First-Principle Calculations

Can Ding, Xing Hu, and Lu Feng

College of Electrical Engineering &New Energy, China Three Gorges University, Yichang 443002, China

Correspondence should be addressed to Xing Hu; huxing@ctgu.edu.cn

Received 8 December 2021; Accepted 5 March 2022; Published 27 March 2022

Academic Editor: Gayanath Fernando

C_4F_7N, $C_5F_{10}O$, etc., as new environmental-friendly alternative gases decompose under partial discharge and produce a series of products such as CO, CF_4, C_2F_6, C_3F_8, CF_3CN, C_2F_5CN, and COF_2. Based on the first-principles calculation method of density functional theory (DFT), the adsorption characteristics of intrinsic state graphene and Mo-doped graphene adsorbing SF_6 and its substitute gas decomposition products are calculated and analyzed. By comparing the adsorption energy, adsorption distance, density of state, Mulliken charge population, charge transfer amount, and molecular orbital energy for adsorbing different decomposition gases, it can be seen that the system structure is the most stable when Mo is doped at the T site of the graphene surface. The adsorption of Mo-doped graphene on gas molecules is significantly stronger than that of intrinsic graphene, and the order of adsorption is: $SO_2F_2 > H_2S > SO_2 > CF_4$. The adsorption of H_2S gas molecules by intrinsic state and Mo-doped graphene is n-type adsorption, while the adsorption of SO_2F_2, CF_4, and SO_2 gas molecules is p-type adsorption. Mo-doped graphene can be used as a detection device for SO_2F_2 gas resistance sensors.

1. Introduction

Sulfur hexafluoride (SF_6) gas is widely used in direct current breakers and gas insulated switchgear (GIS) due to its excellent insulation performance and arc extinguishing performance [1–4]. However, SF_6 gas insulation device will inevitably leak in the process of installation, use, and commissioning. Because of its great greenhouse effect and extremely difficult decomposition in the atmosphere, scientists and scholars from all over the world began to study new SF_6 alternative gas. The research results show that C_4F_7N, $C_5F_{10}O$, CF_3I, and other new environmental-friendly gases can replace SF_6 gas to a certain extent [5–8]. However, during long-term use, certain defects, and aging phenomena will inevitably occur in electrical equipment, resulting in a decline in its insulation performance, resulting in spark discharge or thermal breakdown under the action of the arc, which will decompose SF_6 and its new alternative gas. The decomposed gas will react with a small amount of carbon dioxide and water in electrical equipment and other trace substances, and then generate a variety of harmful gases to the environment, such as CF_4, SO_2F_2, SO_2, and H_2S [9–11] (Figure 1). These decomposition gases are not only harmful to the environment but also threaten the safety of workers and the normal and stable operation of electrical equipment. With the national "carbon peak and carbon neutral" goal proposed, environmental-friendly operation and management of electrical equipment has become a general trend [12]. Therefore, it is essential to monitor and analyze the decomposition products of SF_6 gas.

In recent years, with the continuous in-depth research on semiconductor sensor materials, various types of gas sensors have attracted extensive attention. Zhang et al. [13] show that Ni-doped In_2O_3/WS_2 nanohybrid materials provide a new way for formaldehyde sensors. Another study Zhang et al. [14] found that Ni-doped MoS_2 films can be used as SO_2 gas sensors. Also, another study by Zhang et al. [15] show that ZnO/WS_2 nanoheterostructures can detect

trace benzene gas at room temperature. Based on the first-principles calculations of density functional theory, it is believed that Au-doped $MoSe_2$ composites are more beneficial as NH_3 gas sensors [16]. Graphene is a new type of carbon nanofunctional material constructed by layers of carbon atoms. Similar to other inorganic oxide semiconductor metal oxides (CuO, Co_3O_4, SnO_2, In_2O_3, and $LaFeO_3$) gas sensors, graphene not only has low cost [17], large surface area [18], high stability, good electrical conductivity [19], high mechanical strength [20], high carrier mobility [21], and a series of advantages but also in gas adsorption has a wider application. Pearce et al. [22] studied the adsorption of individual gas molecules by intrinsic graphene and found that intrinsic graphene only has good gas sensitivity to a small part of gas molecules such as NH_3 and NO_2. It can be seen that intrinsic graphene because of its very stable structure and no dangling bonds, there are obvious limitations in the adsorption of gas molecules. Relevant studies have shown [23] that doping can improve the adsorption characteristics of intrinsic graphene for specific gases. Sun et al. [24] calculated the adsorption of O, O_2, OH, and OOH by B-P atom single doping and codoping graphene and found that codoping has a synergistic effect and the adsorption effect is the best. Song et al. [25] comparatively analyzed the adsorption of C_2H_4 gas on graphene doped with Fe, Co, and Ni based on density functional theory and found that Ni-doped graphene has the best adsorption capacity. Wang et al. [26] used B, P, Pd, and Pt single-doped graphene to adsorb H_2 and CO gases, respectively, and the results showed that the single-doped Pd and Pt graphene had a better adsorption effect on these two gases. Zhang et al. [27] found that the surface of Au-doped graphene has good gas sensitivity to SO_2F_2 gas molecules based on simulations and experiments.

At present, although there have been some studies on the adsorption of gas molecules on the surface of element-doped graphene, most of the adsorbed gas molecules are conventional gases such as NH_3 and CO_2, and the research used to detect the decomposition products of SF_6 and its substitute gas is still very rare. Therefore, this paper is based on density functional theory (DFT) [28], using first-principle calculation methods to explore the four gas molecules of H_2S, SO_2, CF_4, and SO_2F_2 in Mo-doped graphite. The adsorption parameters, the density of states, the Mulliken charge population, the amount of charge transfer, and the energy of the molecular orbital on the surface of the alkene provide a theoretical basis for the study of high-performance gas sensors to monitor the decomposition products of SF_6 and its substitute gases.

2. Calculation Parameter Design

The calculation of this paper mainly uses DMol3 module. First, select a single-layer graphene cell with lattice constant $a = b = 0.246$ nm, $c = 0.680$ nm, crystal plane angle $\alpha = \beta = 90^\circ$, $\gamma = 120^\circ$, a total of two carbon atoms, and then expand 6 times in the a and b directions to create a 6×6 supercell with 72 carbon atoms in total. Take a 20 Å vacuum layer in the c direction of the unit cell to prevent mutual

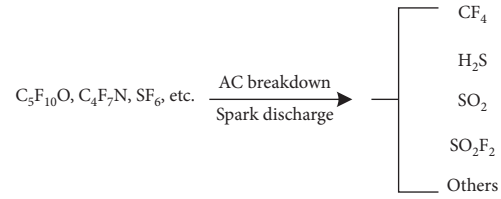

Figure 1: SF_6 and its substitute gas decomposition product process.

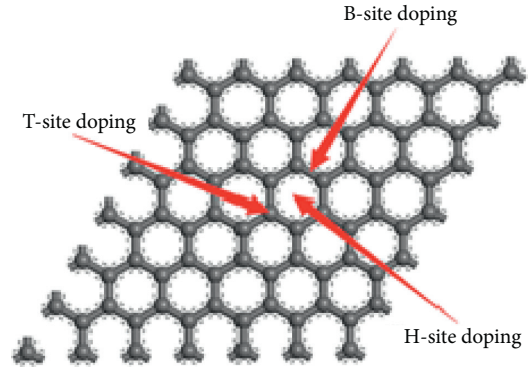

Figure 2: Three possible Mo doping positions.

interference between adjacent layers of graphene during the optimization process, thereby affecting the accuracy of the calculation results. The bond length between carbon-carbon bonds in the graphene structure is 0.142 nm, and the theoretical thickness of a single layer of atoms is 0.34 nm.

In this paper, the PBE (Perdew, Burke, and Ernzerhof) basis set of the generalized gradient approximation (GGA) is used to deal with the exchange correlation energy between atoms [29], and the intrinsic state graphene and Mo-doped graphene unit cells are analyzed respectively. Optimize the geometric structure to obtain a stable geometric structure, and then calculate the adsorption process of the four typical decomposition gases for the stable geometric structure to find the most stable adsorption structure, and finally analyze the calculated results to find the best adsorption capacity gas sensor. Set the grid space k points to $6 \times 6 \times 1$. In the adsorption model, consider the obvious role of van der Waals force in the physical adsorption effect. To achieve more accurate calculation results, the DFT-D used to correct the dispersion force is added during the iteration process (Tkatchenk and Scheffler, TS) algorithm [30], set the orbital cut-off radius 3.5 Å, the single-atom energy convergence accuracy during the iteration process, the maximum stress, the maximum displacement between atoms, the convergence standards are 1.0×10^{-5}Ha, 0.004Ha/Å and 0.005 Å, respectively, Consider spin polarization.

3. Results and Discussion

3.1. Binding Energy Analysis. The graphene crystal structure has high periodicity and symmetry. Therefore, there are three kinds of doping at different positions during the doping process, namely, the top position T (directly above the carbon atom), doping, and the bridge position B (two

Table 1: Doping formation energy of Mo-Graphene surface.

Models	$E_f(T)$ (eV)	$E_f(B)$ (eV)	$E_f(H)$ (eV)
Mo-Gra	0.75	1.36	1.49

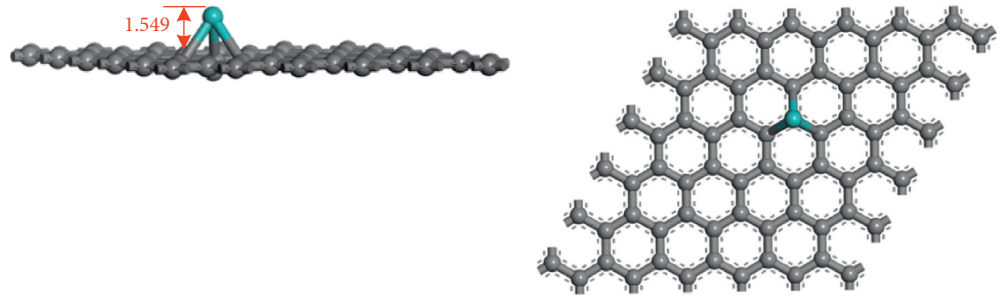

(a) (b)

Figure 3: Mo doping site: (a) Side view and (b) top view.

doped with a carbon atom in the middle), and doped with an acupuncture point H (in the center of the carbon ring), as shown in Figure 2.

The most stable adsorption structure can be determined by the size of the binding energy. The smaller the binding energy, the more stable the adsorption structure. The formula for the binding energy (E_{form}) of Mo atom-doped graphene surface is as follows:

$$E_{binding} = E_{Mo-Gra} - E_{Gra} - E_{Mo}. \quad (1)$$

Among them, $E_{binding}$ is the binding energy of Mo atom-doped graphene structure, $E_{Mo\text{-}Gra}$ is the energy when the entire doping system is most stable after Mo atoms doping the graphene surface, E_{Gra} is the total energy of intrinsic graphene, and E_{Mo} is the total energy of a single Mo atom. By comparing the size of the binding energy, the most stable adsorption structure for gas molecule adsorption can be obtained. The binding energy of different positions of Mo atom-doped graphene is shown in Table 1. It can be seen from Table 1 that in the three different doping processes, the binding energy is the lowest when Mo atoms are doped to replace the carbon atoms in the T position of graphene. It can be seen that the structure model after T position doping is more stable. It is also easier to form. Therefore, the adsorption calculations of SF6 and its substitute gas decomposition products later in this article are based on the structural model of B-Au doped T-site graphene.

The side view and top view of the Mo atom-doped intrinsic graphene surface are shown in Figures 3(a) and 3(b). It can be seen from Figure 3 that after Mo atoms doped the intrinsic graphene surface, the intrinsic graphene surface structure did not change significantly, but because the radius of Mo atoms is much larger than that of C atoms and the local sp^3 formed near the Mo atoms after doping hybrid configuration, the Mo atom and the surrounding three adjacent C atoms form a covalent bond, and the Mo atom protrudes directly above, the protruding height is about 1.549 Å, and the C-Mo bond length is 2.02 Å, this is similar to the structure studied in the literature, so the model calculated in this article is correct and reliable and can be used to calculate other properties.

3.2. Adsorption Performance Analysis. First, optimize the structure of SF_6 and its substitute gas decomposition products, and then perform adsorption calculations on the optimized gas molecules and Mo-doped intrinsic graphene surface. Set the initial adsorption distance to 2 Å. Figure 4 is the structural model of the optimized gas molecules, and Figures 5(a) and 5(b) are the most stable structural models of the gas molecules adsorbed on the eigenstate and Mo atom-doped intrinsic graphene surface, respectively.

In order to analyze the adsorption characteristics of SF_6 and its substitute gas decomposition products on the surface of different atom-doped graphene, the energy change value of the adsorption process between the different atom-doped T-site graphene surface and the SF_6 decomposition gas is introduced, which is the adsorption energy ($\triangle E_{ads}$) [31]:

$$\Delta E_{ads} = E_{gas-Mo-Gra} - E_{Mo-Gra} - E_{gas}. \quad (2)$$

Among them, $E_{gas\text{-}Mo\text{-}Gra}$ is the total energy of Mo atom-doped graphene surface adsorbed gas molecules, $E_{Mo\text{-}Gra}$ is the total energy of Mo atom-doped graphene surface, and E_{gas} is the total energy of gas molecules. The positive or negative of the adsorption energy indicates whether the reaction is exothermic or endothermic. The absolute value of the adsorption energy indicates the strength of the adsorption capacity. The larger the absolute value, the stronger the adsorption capacity.

Table 2 shows the adsorption energy ($\triangle E_{ads}$), adsorption distance (d), and bond length (Å) of the four gas molecules decomposed by SF_6 and its substitute gas. As can be seen from Table 2, as for the adsorption energy, intrinsic graphene has weak adsorption capacity for four kinds of gas molecules but strong adsorption capacity for H_2S gas, while Mo-doped graphene surface has increased adsorption capacity for four kinds of gas molecules, and has the strongest adsorption capacity for SO_2F_2 gas. According to Zhou et al.

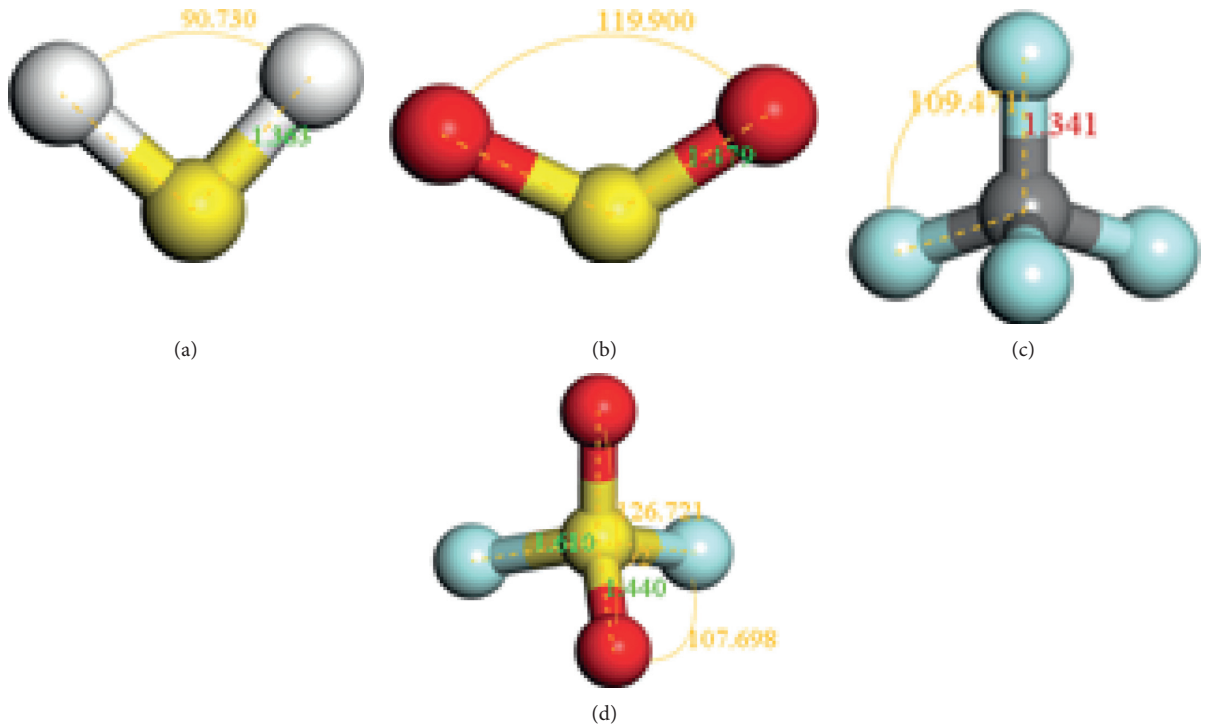

Figure 4: Optimized gas model: (a) H_2S, (b) SO_2, (c) CF_4, and (d) SO_2F_2.

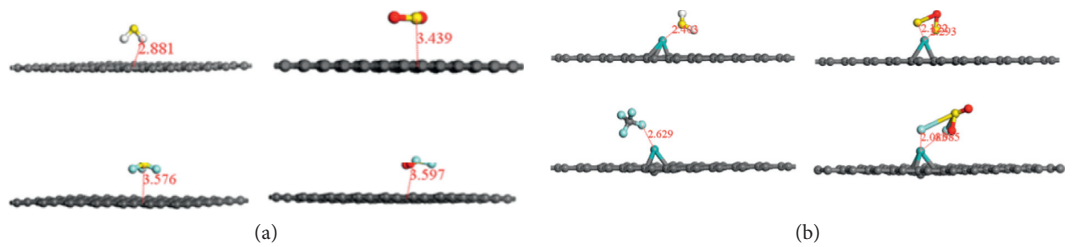

Figure 5: The most stable model of SF_6 decomposition gas adsorption: (a) grapheme and (b) Mo-doped graphene.

[32], when the adsorption energy is greater than 0.8 eV, the adsorption effect is chemical adsorption, and vice versa, it is physical adsorption. It can be seen from the data in the table that the adsorption capacity of intrinsic graphene for these four gas molecules is relatively weak, all of which are physical adsorption; while the adsorption of SO_2 and CF_4 on the surface of Mo-doped graphene is still physical adsorption., the effect is not obvious, but the adsorption of H_2S and SO_2F_2 gas molecules is chemical adsorption, and the interaction is relatively strong. As for the adsorption distance, the eigenstate graphene adsorbs H_2S gas molecules the shortest distance, and the Mo-doped graphene surface adsorbs SO_2F_2 gas molecules the shortest distance. The shorter the adsorption distance, the stronger the interaction, which also corresponds to the adsorption energy. Regarding the bond length, after the intrinsic graphene adsorbs the four gas molecules, the bond length between the atoms in the gas molecules hardly changes, and the intrinsic graphene and the four gas molecules are also reacted from the side. The interaction between them is relatively weak, and after the Mo-doped graphene surface adsorbs these four gas molecules, the bond length between the atoms in the gas molecules has changed significantly, especially the SO_2 and SO_2F_2 gas molecules, which adsorb SO_2 gas. After the molecule, the bond lengths of the two S-O bonds were extended to 3.639 Å and 1.529 Å, respectively. After the SO_2F_2 gas was adsorbed, the bond lengths between the two S-F bonds were 3.431 Å and 2.969 Å, respectively, indicating that the S-F bond has been broken and the SO_2F_2 gas molecule has cracked, indicating that a strong chemical reaction occurred between the SO_2F_2 gas and the Mo-doped graphene surface.

To more clearly show the changes in the surface structure parameters of the intrinsic graphene and Mo-doped graphene before and after adsorption. Figures 6(a) and 6(b) shows the adsorption energy and adsorption distance of the four gases in different graphene structures. It can be seen from Figure 6 that the absolute value of the adsorption energy of the intrinsic state graphene for the four gas molecules is $H_2S > SO_2F_2 > CF_4 > SO_2$ and the adsorption distance is $SO_2 > CF_4 > SO_2F_2 > H_2S$, Mo doped the adsorption energy of intrinsic graphene

Table 2: Adsorption parameters of SF_6 and its substitute gas decomposition products on the surface of intrinsic graphene and Mo-doped T-site graphene.

Models	$\triangle E_{ads}$ (eV)	d (Å)	Bond length (Å)
Graphene/(H_2S)	−0.617	2.881	1.355 (S-H_1) 1.356 (S-H_2)
Mo-Graphene/(H_2S)	−0.986	2.403	1.372 (S-H_1) 1.374 (S-H_2)
Graphene/(SO_2)	−0.302	3.439	1.482 (S-O_1) 1.479 (S-O_2)
Mo-Graphene/(SO_2)	−0.653	2.176	3.639 (S-O_1) 1.529 (S-O_2)
Graphene/(CF_4)	−0.409	3.576	1.341 (C-F_1) 1.340 (C-F_1)
Mo-Graphene/(CF_4)	−0.421	2.629	1.543 (C-F_1) 1.542 (C-F_2)
Graphene/(SO_2F_2)	−0.472	3.597	1.611 (S-F_1) 1.609 (S-F_2) 1.440 (S-O_1) 1.441 (S-O_2)
Mo-Graphene/(SO_2F_2)	−1.653	2.035	3.431 (S-F_1) 2.969 (S-F_2) 1.497 (S-O_1) 1.597 (S-O_2)

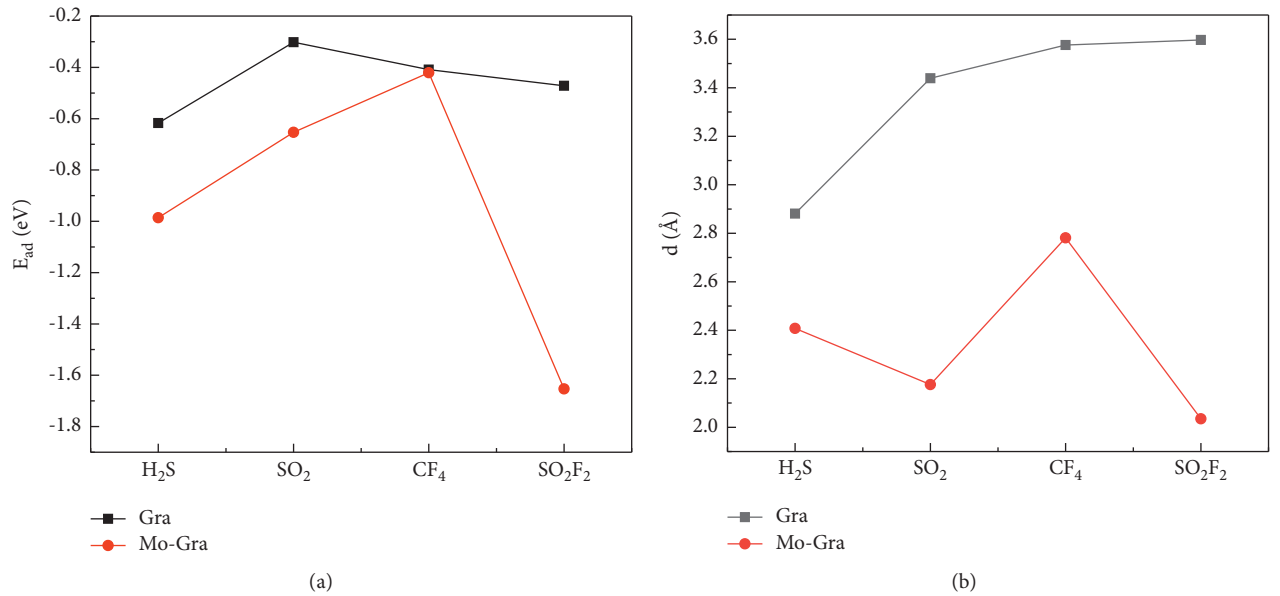

Figure 6: Adsorption properties of H_2S, SO_2, CF_4, and SO_2F_2 in different graphene structures: (a) adsorption energies and (b) adsorption distances.

for the four decomposition gases is $SO_2F_2 > H_2S > SO_2 > CF_4$, and the absolute value of charge transfer is $CF_4 > SO_2 > H_2S > SO_2F_2$.

From the calculation and analysis of the above adsorption parameters, it can be seen that the Mo-doped intrinsic graphene has the strongest ability to adsorb SO_2F_2 gas molecules. Therefore, this article mainly takes the adsorption of SO_2F_2 gas as an example to further explore the adsorption characteristics of SF_6 decomposition gas on the surface of Mo-doped graphene.

3.3. Density of State Analysis. To further analyze the influence of Mo-doped graphene surface on the adsorption characteristics of SF_6 and its substitute gas decomposition products, this paper analyzes the total density of states and atomic partial wave states of intrinsic graphene and Mo-doped intrinsic graphene adsorbed SO_2F_2 gas molecules on the surface. The density was calculated and analyzed. Since the region far away from the Fermi level has little effect on the properties of the system and can be ignored, this paper mainly selects the density of states in

the range of −24 eV~4 eV for analysis. Figure 7(a) shows the calculated total spin state density of the intrinsic state graphene and Mo-doped graphene adsorbed SO_2F_2 gas molecules, and Figure 7(b) shows the partial waves of Mo, S, F, O, and C atoms. Spin state density: it can be seen from Figure 7(a) that the intrinsic graphene spin-up state density and spin-down state density coincide near the Fermi level, and the Fermi level passes through the Dirac point, indicating that the intrinsic graphene is graphene. It is a direct band gap semiconductor, which is consistent with the results obtained in [33]. After the surface of graphene is doped with Mo atoms, there is overlap between the bottom of the conduction band and the top of the valence band, which shows the characteristics of the metal, and the density of state has changed to a certain extent, which shows that the doped Mo atoms have a certain influence on the adsorption substrate. After adsorption of SO_2F_2 gas molecules, the spin state density of intrinsic graphene basically coincides with that before adsorption, with little change, which reflects that the adsorption of intrinsic graphene to SO_2F_2 gas molecules is not strong, while the spin state density of Mo-doped graphene shifts to the right as a whole, which indicates that its conductivity becomes stronger, and the state density changes greatly near its Fermi level ($E_f = 0$ eV) and at the top of valence band and at the bottom of conduction band, which also reflects the adsorption of Mo-doped graphene to SO_2F_2 gas molecules. Figure 7(b) shows the local spin state density. After Mo-doped graphene adsorbs SO_2F_2 gas molecules, the state density near the Fermi level is mainly composed of Mo-4d and S-3p orbitals, and the density of states with energy of −8 eV ~ −4 eV is mainly composed of Mo-4d, O-2p, F-2p, C-2p, and S-3p orbitals, and in this energy domain, there is overlapping hybridization between Mo-4d and S-3p orbitals, and Mo-4d and F-2p orbitals overlap to some extent at energy of −1 eV~2 eV. It can be seen that it is precisely.

3.4. Analysis of Mulliken Population and Transfer Charge. Table 3 shows the orbital charge distribution of SO_2F_2 gas molecules adsorbed by Mo atom-doped graphene. As can be seen from Table 3, the total charge numbers of Mo atoms and S atoms are 1.028*e* and 0.448*e*, respectively, which are positively charged and lose electrons, while O atoms and F atoms are negatively charged and gain electrons, which indicates that when the surface of Mo-doped intrinsic graphene adsorbs SO_2F_2 gas molecules, the fracture of S-F is mainly caused by the hybridization between molecular orbitals, which is also consistent with the analysis results of the density of spin states.

According to Bader's charge analysis [34], the charge amount of a single atom in different systems can be calculated, and the charge transfer amount of the whole system can be obtained by subtracting the charge amount of the system after doping or adsorption of atoms (molecules) from the charge amount of the system before doping or adsorption.

$$\Delta Q = Q_1 - Q_2, \tag{3}$$

where $\triangle Q$ is the charge transfer amount of the system before and after doping or adsorption, $\triangle Q_1$ is the charge amount of the system after doping or adsorption, and $\triangle Q_2$ is the charge amount of the system before doping or adsorption. If the charge transfer amount is greater than 0, then, the system loses electrons in the doping or adsorption process, and the doping or adsorption substrate is the acceptor, otherwise, it means that the system gets electrons in the doping or adsorption process, and the doping or adsorption substrate is the donor. Table 4 shows the transfer charge amounts of four kinds of gas molecules on the surface of intrinsic graphene and Mo-doped intrinsic graphene.

According to the charge transfer amount in Table 4, only the surface of intrinsic graphene and Mo-doped intrinsic graphene has a positive transfer charge when adsorbing H_2S gas molecules, while the others are all negative, which indicates that when the surface of intrinsic graphene and Mo-doped intrinsic graphene adsorbs H_2S gas molecules, H_2S gas transfers electrons to the substrate, while the surface of intrinsic graphene and Mo-doped intrinsic graphene acts as a collector and H_2S gas molecules act as a donor. On the contrary, the surface of intrinsic graphene and Mo-doped intrinsic graphene acts as a donor when adsorbing other gases and transfers electrons to other gases.

3.5. Molecular Orbital Energy Analysis. According to the molecular orbital theory [35], the charge transfer is directly related to the direction of molecular energy level change. To further study the principle of charge transfer during adsorption, in this paper, the highest orbital (HOMO) occupied the energy and the lowest orbital (LUMO) occupied the energy of these four gas molecules, the energy of intrinsic graphene Fermi level ($E_f = -4.338$ eV), and the energy of Mo-doped intrinsic graphene Fermi level ($E_{f\text{-}Mo} = -3.993$ eV) are calculated, respectively. $E_{\text{f-L}}$ or $E_{\text{f-Mo-L}}$, respectively, represents the difference between LUMO molecular orbital energy of four gas molecules and Fermi energy level of intrinsic graphene or Mo-doped graphene. Similarly, $E_{f\text{-}H}$ or $E_{f\text{-}Mo\text{-}H}$, respectively, represents the difference between HOMO molecular orbital energy of four gas molecules and Fermi energy level of intrinsic graphene or Mo-doped graphene. The electron cloud distribution of four gas molecules is shown in Figure 8.

Among them, $E_0 = E_{\text{LUMO-EHOMO}}$ is the orbital energy gap of gas molecules, which mainly reflects the energy needed when gas molecules react with other substances. It can be seen from Figure 8 that the orbital gaps of four kinds of gas molecules from small to large are $CF_4 > SO_2F_2 > H_2S > SO_2$, the maximum orbital gap of CF_4 gas molecules is 12.495 eV, and the minimum orbital gap of SO_2 gas molecules is 5.642 eV. It can be calculated that the energy differences $E_{f\text{-}L}$ between the HOMO-LUMO energy levels of H_2S, SO_2F_2, CF_4, and SO_2 and the Fermi energy levels of intrinsic graphene are 4.131 eV, 0.532 eV, 4.217 eV, 3.269 eV, 2.759 eV, 1.304 eV, 8.157 eV, and 4.512 eV, respectively. The energy difference between $E_{f\text{-}L}$ and Mo-

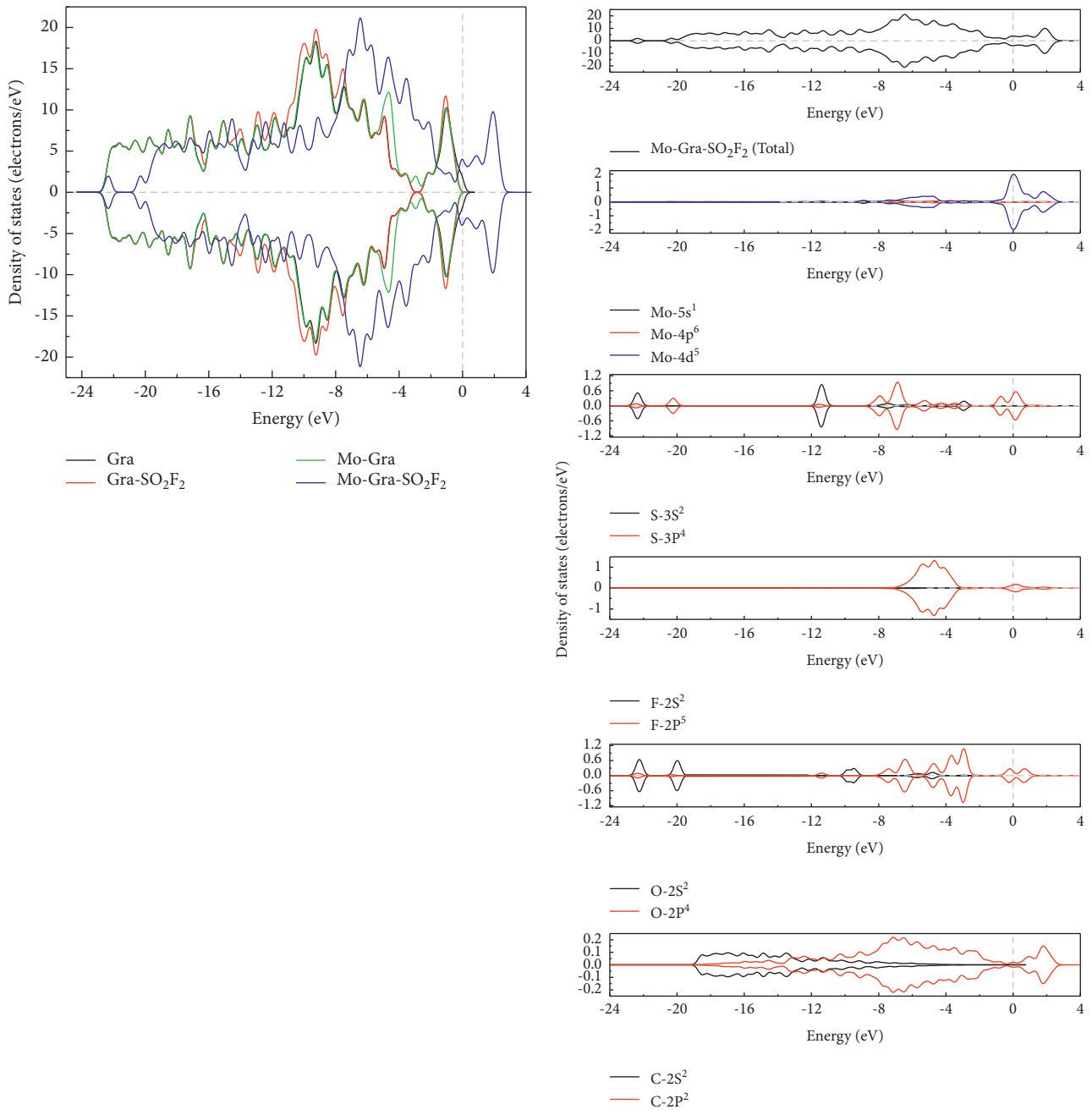

Figure 7: Density of states: (a) density of spin states before and after adsorption of SO_2F_2 on intrinsic graphene and Mo-doped grapheme and (b) Mo-doped graphene adsorption of SO_2F_2 gas molecule spin state density of each atom.

Table 3: The orbital charge distribution of SO_2F_2 gas molecules adsorbed by Mo-doped intrinsic graphene.

Atoms	S track (e)	P track (e)	D track (e)	Electric charges (e)
Mo	1.186	3.161	2.093	1.119
S	2.913	4.549	0.313	0.450
O_1	1.927	2.265	0.018	−0.420
O_2	1.921	2.210	0.019	−0.300
F_1	1.995	2.739	0.006	−0.479
F_2	1.996	2.738	0.006	−0.480

Table 4: Transfer charge of gas molecules on the surface of intrinsic graphene and Mo-doped intrinsic graphene.

Models	Transfer charge ($\triangle Q$)
Graphene/(H_2S)	+0.010
Mo- Graphene/(H_2S)	+1.348
Graphene/(SO_2)	−0.011
Mo- Graphene/(SO_2)	−0.345
Graphene/(CF_4)	−0.013
Mo- Graphene/(CF_4)	−0.215
Graphene/(SO_2F_2)	−0.004
Mo- Graphene/(SO_2F_2)	−0.952

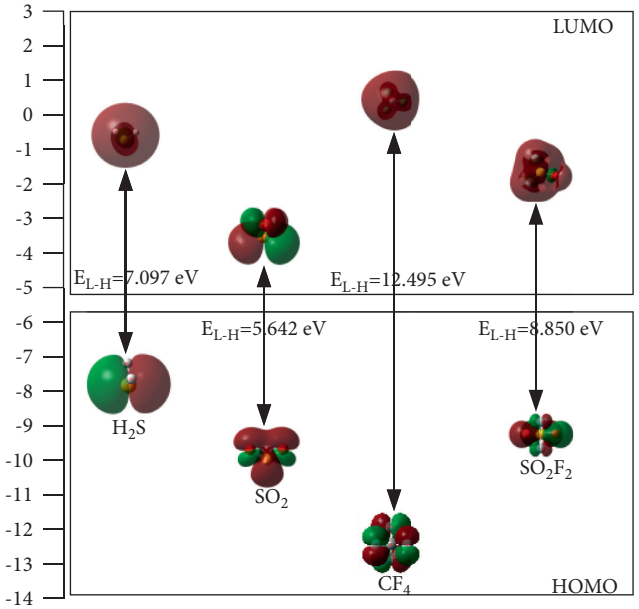

Figure 8: Molecular orbital gap value of H_2S, SO_2, CF_4, and SO_2F_2.

doped intrinsic graphene Fermi level is 3.786 eV, 0.187 eV, 3.872 eV, 2.924 eV, $E_{f\text{-}H}$ is 3.311 eV, 5.455 eV, 8.502 eV, and 4.857 eV. It can be seen from the calculation results that among the four kinds of gas molecules, whether intrinsic graphene or Mo-doped graphene, only $E_{F\text{-}H}$ of H_2S gas is less than $E_{F\text{-}L}$, that is, the energy difference between HOMO of H_2S and the work function $\varphi_{Mo\text{-}Gra}$ of Mo-doped graphene is less than the energy difference between LUMO and $\varphi_{Mo\text{-}Gra}$ [36], which indicates that in the process of adsorbing H_2S gas, the surfaces of intrinsic graphene and Mo-doped graphene are current collectors, and H_2S gas is donor. However, $E_{F\text{-}H}$ of SO_2F_2, CF_4, and SO_2 is greater than $E_{F\text{-}L}$, and the adsorption process with intrinsic graphene and Mo-doped graphene is all P-type adsorption, and the surfaces of intrinsic graphene and Mo-doped graphene are donors and gas molecules are acceptors, which is also consistent with the analysis results of transfer charge.

4. Conclusion

In this work, we discuss the interaction between SF_6 decomposition products (H_2S, SO_2, CF_4, and SO_2F_2) with intrinsic graphene and Mo-doped graphene, considering whether there is the effect of Mo atom doping. It was found that the doped architecture was the most stable when Mo atoms were doped at the T sites of graphene. Intrinsic graphene does not have strong adsorption of H_2S, SO_2, CF_4, and SO_2F_2, these four SF_6 decomposition gases, all of which are physical adsorption, while Mo-doped graphene surface has enhanced adsorption capacity for the four gases. Also, the adsorption strength is $SO_2F_2 > H_2S > SO_2 > CF_4$. After Mo-doped graphene surface, the overall density of states of the system shifts, the conductivity becomes stronger, and orbital hybridization occurs between F, S atoms, and Mo atoms in SO_2F_2 gas, which leads to the breaking of SF bonds and also makes adsorption the most obvious effect. According to the direction of electron transfer and molecular orbital energy, the adsorption of H_2S gas molecules on the surface of Mo-doped graphene is n-type adsorption, while the adsorption of SO_2F_2, CF_4, and SO_2 gas molecules is p-type adsorption. This study theoretically demonstrates that the Mo-doped graphene surface can be used as a detection device for H_2S and SO_2F_2 gas scavengers and SO_2F_2 gas resistance sensors, which is of great significance for maintaining the safe and stable operation of power systems.

Data Availability

The data used to support the findings of this study are included within the article.

Conflicts of Interest

The authors have no conflicts of interest.

References

[1] D. Xiao, D. Yue, and D. Huang, "GIS technology of UHV transmission project in China," *High voltage technology*, vol. 32, no. 12, pp. 115–117, 2006.

[2] Y. Li, X. Zhang, Z. Cui, H. Xiao, and G. Zhang, "Experimental study on the effect of NH_3 on the degradation of SF_6 by DBD," *Journal of Electrical Technology*, vol. 34, no. 24, pp. 5262–5269, 2019.

[3] Z. Zhou, H. Dong, M. Zhao, and G. Zhang, "Summary of research on decomposition characteristics of SF_6 substitute gas," *Journal of Electrotechnical Technology*, vol. 35, no. 23, pp. 4998–5014, 2020.

[4] G. Wei, Y. Bai, M. Hu, Z. Cao, and W. Fu, "Research on environmental protection treatment for ex-service SF6 adsorbent," *IEEE Access*, vol. 8, pp. 93840–93849, 2020.

[5] M. Xiao, X. Feng, X. Li, R. Gao, and B. Du, "Effect of micro-H_2O and micro-O_2 on the decomposition characteristics of insulating medium C3F7CN gas using molecular dynamics and transition state method," *Journal of Molecular Modeling*, vol. 26, no. 9, p. 252, 2020.

[6] Y. Zhang, X. Zhang, Y. Li et al., "AC breakdown and decomposition characteristics of environmental friendly gas C5F10O/air and C5F10O/N2," *IEEE Access*, vol. 7, pp. 73954–73960, 2019.

[7] Z. Zhou, H. Dong, and M. Zhao, "Decomposition characteristics of $C_5F_{10}O$ mixture under corona discharge," *Transactions of China Electrotechnical Society*, vol. 36, no. 2, pp. 407–416, 2021.

[8] X. Yan, Y. Zheng, and H. Huang, "Sensitivity of C_4F_7N/CO_2 gas mixture to partial inhomogeneous electric field," *Transactions of China Electrotechnical Society*, vol. 35, no. 1, pp. 43–51, 2020.

[9] F. Zeng, J. Tang, and Y. Qiu, "The formation of SF6 decomposition components by micro-water under partial discharge and its influence rule," in *Proceedings of the 2012 Academic Conference of Chongqing Electrical Engineering Society*, pp. 945–951, Chongqing Electrical Engineering Society, Chongqing, China, 2012.

[10] H. Sun, *Study on the Influence of Micro-water and Micro-oxygen on SF_6 Decomposition Characteristics under Overheating Fault*, Chongqing University, Chongqing, China, 2014.

[11] D. Chen, X. Zhang, H. Xiong et al., "A first-principles study of the SF6 decomposed products adsorbed over defective WS2 monolayer as promising gas sensing device," *IEEE Transactions on Device and Materials Reliability*, vol. 19, no. 3, pp. 473–483, 2019.

[12] Y. Li, X. Zhang, M. Fu, S. Xiao, J. Tang, and S. Tian, "Research and application progress of environmental protection insulating gas C_4F_7N I: insulation and electrical and thermal decomposition characteristics," *Journal of Electrotechnical Technology*, vol. 36, no. 17, pp. 3535–3552, 2021.

[13] D. Zhang, Y. Cao, Z. Yang, and J. Wu, "Nanoheterostructure construction and DFT study of Ni-doped In2O3 nanocubes/WS2 hexagon nanosheets for formaldehyde sensing at room temperature," *ACS Applied Materials & Interfaces*, vol. 12, no. 10, pp. 11979–11989, 2020.

[14] D. Zhang, J. Wu, P. Li, and Y. Cao, "Room-temperature SO2 gas-sensing properties based on a metal-doped MoS2 nanoflower: an experimental and density functional theory investigation," *Journal of Materials Chemistry*, vol. 5, no. 39, pp. 20666–20677, 2017.

[15] D. Zhang, J. Wu, P. Li, Y. Cao, and Z. Yang, "Hierarchical nanoheterostructure of tungsten disulfide nanoflowers doped with zinc oxide hollow spheres: benzene gas sensing properties and first-principles study," *ACS Applied Materials & Interfaces*, vol. 11, no. 34, pp. 31245–31256, 2019.

[16] D. Zhang, Z. Yang, P. Li, M. Pang, and Q. Xue, "Flexible self-powered high-performance ammonia sensor based on Au-decorated MoSe2 nanoflowers driven by single layer MoS2-flake piezoelectric nanogenerator," *Nano Energy*, vol. 65, Article ID 103974, 2019.

[17] D. Zhang, W. Pan, L. Zhou, and S. Yu, "Room-Temperature benzene sensing with Au-doped ZnO nanorods/exfoliated WSe2 nanosheets and density functional theory simulations," *ACS Applied Materials & Interfaces*, vol. 13, no. 28, pp. 33392–33403, 2021.

[18] M. D. Stoller, S. Park, Y. Zhu, J. An, and R. S. Ruoff, "Graphene-based ultracapacitors," *Nano Letters*, vol. 8, no. 10, pp. 3498–3502, 2008.

[19] P. Avouris, Z. Chen, and V. Perebeinos, "Carbon-based electronics," *Nature Nanotechnology*, vol. 2, no. 10, pp. 605–615, 2007.

[20] K. S. Novoselov, A. K. Geim, S. V. Morozov et al., "Electric field effect in atomically thin carbon films," *Science*, vol. 306, no. 5696, pp. 666–669, 2004.

[21] K. Nomura and A. H. Macdonald, "Quantum transport of massless Dirac fermions in graphene," *Physical Review Letters*, vol. 98, no. 7, Article ID 076602, 2007.

[22] R. Pearce, T. Iakimov, M. Andersson, L. Hultman, A. L. Spetz, and R. Yakimova, "Epitaxially grown graphene based gas sensors for ultra sensitive NO2 detection," *Sensors and Actuators B: Chemical*, vol. 155, no. 2, pp. 451–455, 2011.

[23] S. Li, G. Chen, H. Ye et al., "Sulfur dioxide molecule sensors based on zigzag graphene nanoribbons with and without Cr dopant," *Physics Letters A*, vol. 378, no. 7-8, pp. 667–671, 2014.

[24] J. Sun, K. Zhou, and X. Liang, "density functional study on adsorption characteristics of O, O_2, OH and OOH by single-doped and co-doped graphene," *Acta Physica Sinica*, vol. 65, no. 1, pp. 391–401, 2016.

[25] S. Song, N. Jia, T. Gong, H. Zhou, and R. Wu, "First-principles study on C_2H_4 adsorption on graphene surface doped with Fe, Co and Ni," *Acta Atomic and Molecular Physics*, vol. 36, no. 4, pp. 710–716, 2019.

[26] L. Wang, W. Li, Y. Cai et al., "Characterization of Pt- or Pd-doped graphene based on density functional theory for H2 gas sensor," *Materials Research Express*, vol. 6, no. 9, Article ID 095603, 2019.

[27] X. Zhang, R. Huang, Y. Lei, X. Dong, and Y. Gui, "Gas-sensitive analysis of SF_6 decomposition components by gold-doped graphene based on first-principles," *Journal of China Electrical Engineering*, vol. 37, no. 6, pp. 1828–1835, 2017.

[28] B. Delley, "From molecules to solids with the DMol3 approach," *The Journal of Chemical Physics*, vol. 113, no. 18, pp. 7756–7764, 2000.

[29] Q. Hou, C. Zhao, J. Li, and G. Wang, "First-principles study on the effect of high doping concentration of Al on the conductivity of ZnO," *Acta Physica Sinica*, vol. 60, no. 4, pp. 571–576, 2011.

[30] S. Pier Luigi, "Van der Waals interactions in DFT made easy by Wannier functions," *Physical Review Letters*, vol. 100, no. 5, pp. 1135–1140, 2008.

[31] X. Zhang, J. Fang, H. Cui, Y. Gui, and D. Chen, "A summary of the adsorption mechanism of carbon nanotube sensor and its application in detecting SF_6 decomposition components," *Journal of China Electrical Engineering*, vol. 38, no. 16, pp. 4926–4941, 2018.

[32] M. Zhou, Y. Lu, Y. Cai, and C. Zhang, "Adsorption of gas molecules on transition metal embedded graphene: a search for high-performance graphene-based catalysts and gas sensors," *Nanotechnology*, vol. 22, no. 38, Article ID 385502, 2011.

[33] S. Xiao, J. Zhang, X. Zhang, and H. Cui, "Pt-doped single-walled CNT as a superior media for evaluating the operation status of insulation devices: a first-principle study," *AIP Advances*, vol. 8, no. 10, Article ID 105101, 2018.

[34] X. Zhang, J. Wang, D. Chen et al., "Calculation of adsorption properties of Ti-doped MoS_2 to CF_4, C_2F_6 and COF_2 based on first-principles," *High-voltage Electrical Apparatus*, vol. 57, no. 3, pp. 89–96, 2021.

[35] Z. Cao, W. Li, G. Wei, Q. Yao, and G. Hu, "Study on the adsorption characteristics of platinum-doped single-walled carbon nanotubes on the typical decomposition products of the new environmentally friendly gas CF_3I," *Transactions of the Chinese Society of Electrical Engineering*, vol. 36, no. 17, pp. 3564–3571, 2021.

[36] D. Wang, X. Wang, A. Yang et al., "A first principles theoretical study of the adsorption of SF6 decomposition gases on a cassiterite (110) surface," *Materials Chemistry and Physics*, vol. 212, no. 212, pp. 453–460, 2018.